

Optimized Schwarz Methods With Data-Sparse Transmission Conditions

Martin J. Gander and Michal Outrata

1 Introduction and Model Problem

Optimized Schwarz methods (OSMs) use optimized transmission operators between subdomains adapted to the equation to be solved to maximize the convergence rate. OSMs have been studied in detail for *localized* transmission operators, see [6] and references therein, which after discretization become structurally sparse, banded matrices. We consider here *non-localized* transmission operators that become after discretization *data-sparse* matrices – a complementary approach to structural sparsity. Our main focus is on how to optimize OSMs within the classes of data-sparse approximations of the Schur complement.

As model problem we consider the Poisson equation on $\Omega = (-a, a) \times (0, 1) \subset \mathbb{R}^2$,

$$-\Delta u = f \quad \text{in } \Omega, \quad \text{and} \quad u = g \quad \text{on } \partial\Omega, \quad f \text{ and } g \text{ given.} \quad (1)$$

We decompose Ω into two overlapping subdomains $\Omega_1 = (-a, L) \times (0, 1)$ and $\Omega_2 = (-L, a) \times (0, 1)$ with interfaces Γ_1 and Γ_2 , overlap O and complements $\Theta_2 := \Omega_1^c$ and $\Theta_1 := \Omega_2^c$, see Figure 1. Creating an equidistant mesh on Ω with mesh-size h , we denote by N_r the number of grid rows and N_c the number of grid columns, and we discretize (1) with a finite difference scheme, obtaining the block tridiagonal system matrix

$$A = \begin{bmatrix} A_{\Theta_1} & A_{\Theta_1, \Gamma_2} & & & & & & & \\ A_{\Gamma_2, \Theta_1} & A_{\Gamma_2} & A_{\Gamma_2, O} & & & & & & \\ & A_{O, \Gamma_2} & A_O & A_{O, \Gamma_1} & & & & & \\ & & A_{\Gamma_1, O} & A_{\Gamma_1} & A_{\Gamma_1, \Theta_2} & & & & \\ & & & A_{\Theta_2, \Gamma_1} & A_{\Theta_2} & & & & \end{bmatrix}. \quad (2)$$

Martin J. Gander
University of Geneva, e-mail: martin.gander@unige.ch

Michal Outrata
University of Geneva, e-mail: michal.outrata@unige.ch

The POSM iteration matrix T in (3) has the structure¹

$$T = \begin{bmatrix} 0 & K \\ L & 0 \end{bmatrix}, \quad \begin{aligned} K &:= A_{\Omega_1}^{-1} E_{\Gamma_1}^{\Omega_1} \left[I + S_1(A_{\Omega_1}^{-1})_{\Gamma_1, \Gamma_1} \right]^{-1} \left(S_1(E_{\Gamma_1}^{\Omega_2})^T - (E_{\Theta_2}^{\Omega_2})^T \right), \\ L &:= A_{\Omega_2}^{-1} E_{\Gamma_2}^{\Omega_2} \left[I + S_2(A_{\Omega_2}^{-1})_{\Gamma_2, \Gamma_2} \right]^{-1} \left(S_2(E_{\Gamma_2}^{\Omega_1})^T - (E_{\Theta_1}^{\Omega_1})^T \right). \end{aligned} \quad (4)$$

Moreover, the asymptotic convergence factor $\rho(T)$ of POSM satisfies the bound

$$\begin{aligned} \rho(T) &\leq \sqrt{\|M_1 B_1\|_2 \cdot \|M_2 B_2\|_2}, \\ M_1 &:= \left[I + S_1(A_{\Omega_1}^{-1})_{\Gamma_1, \Gamma_1} \right]^{-1} \left(S_1 + A_{\Gamma_1, \Theta_2} A_{\Theta_2}^{-1} A_{\Theta_2, \Gamma_1} \right), \quad B_1 := (A_{\Omega_2}^{-1})_{\Gamma_1, \Gamma_2}, \\ M_2 &:= \left[I + S_2(A_{\Omega_2}^{-1})_{\Gamma_2, \Gamma_2} \right]^{-1} \left(S_2 + A_{\Gamma_2, \Theta_1} A_{\Theta_1}^{-1} A_{\Theta_1, \Gamma_2} \right), \quad B_2 := (A_{\Omega_1}^{-1})_{\Gamma_2, \Gamma_1}. \end{aligned} \quad (5)$$

Remark 1 Because of the symmetry of the subdomains and the problem we have $S_1 = S_2 =: S$, implying² $M_1 = M_2 =: M$ and $B_1 = B_2 =: B$. Notice that both the spectral radius and the norm of T are minimized becoming identically zero by taking for S the exact Schur complement transmission matrix, i.e., $S = S^* := -A_{\Gamma_1, \Theta_2} A_{\Theta_2}^{-1} A_{\Theta_2, \Gamma_1}$.

3 Data-sparse transmission conditions

The term *data-sparse matrix* refers to a low-rank matrix or a matrix with a low-rank structure in some of its blocks. Taking \mathcal{D} as the set of data-sparse matrices of a particular type, e.g., low-rank, we focus on the minimization problem

$$\min_{S \in \mathcal{D}} \|MB\|_2 = \min_{S \in \mathcal{D}} \left\| \left[I + S(A_{\Omega_1}^{-1})_{\Gamma_1, \Gamma_1} \right]^{-1} \left(S + A_{\Gamma_1, \Theta_2} A_{\Theta_2}^{-1} A_{\Theta_2, \Gamma_1} \right) B \right\|_2 \quad (6)$$

$$\leq \min_{S \in \mathcal{D}} \left\| \left[I + S(A_{\Omega_1}^{-1})_{\Gamma_1, \Gamma_1} \right]^{-1} \left(S + A_{\Gamma_1, \Theta_2} A_{\Theta_2}^{-1} A_{\Theta_2, \Gamma_1} \right) B \right\|_F. \quad (7)$$

The Schur complement S^* makes the second term in the norms, the *numerator* part of M , zero but lies in general not in \mathcal{D} . Minimizing only this term over \mathcal{D} might not suffice, since the *denominator* part of M can also play an important role, as shown for structurally sparse transmission conditions in [5, Lemma 5.1, 5.3], [11, Section 2.5, pp. 80]. We call *NumOpt* minimizing the *numerator* part of MB in norm, and *FracOpt* minimizing the *entire expression*. The *NumOpt* solution is in general given by the truncated SVD of S^* or its blocks. For (7) this solution is unique (as the singular values of S^* are distinct), while for (6) we in general don't have uniqueness.

¹ The notation $(A_{\Omega_1}^{-1})_{\Gamma_1, \Gamma_1}$ is an abbreviation for $(E_{\Gamma_1}^{\Omega_1})^T A_{\Omega_1}^{-1} E_{\Gamma_1}^{\Omega_1}$. By analogy we also define $(A_{\Omega_1}^{-1})_{\Gamma_1, \Gamma_2}$ and the counterparts for $A_{\Omega_2}^{-1}$.

² We also use that both A_{Ω_1} and A_{Ω_2} are symmetric Toeplitz matrices and thus their inverses are symmetric and also *persymmetric*, see [7, Section 4.7].

On the other hand, (6) is a sharper bound on the convergence factor. We choose to work with (7) and comment on the differences where appropriate.

A direct computation shows that all the matrices defining M and B in (5), except possibly S_1 and S_2 , can be diagonalized with the *1D discrete Fourier sine basis*

$$W = [\mathbf{w}_1, \dots, \mathbf{w}_{N_r-2}] \text{ with } \mathbf{w}_k = \left[\sin\left(\frac{k\pi}{N_r-1}j\right) \right]_{j=1}^{N_r-2} \in \mathbb{R}^{N_r-2}. \tag{8}$$

We first take S to be a symmetric, rank r matrix of the form

$$S = \sum_{k=1}^r \gamma_k \mathbf{v}_k \mathbf{v}_k^T, \tag{9}$$

where $\gamma \in \mathbb{R} \setminus \{0\}$ and $\mathbf{v}_k \in \mathbb{R}^{N_r-2}$, linearly independent with $\|\mathbf{v}_k\| = 1$. Note that (9) cannot capture the diagonal singularity of S^* well with r small³. Taking

$$\mathbf{v}_k = \mathbf{w}_k \text{ for } k = 1, \dots, r, \tag{10}$$

the matrices M, B can be diagonalized by W , and denoting the spectra by

$$\{\alpha_k\}_1^{N_r-2} := \text{sp}\left((A_{\Omega_1}^{-1})_{\Gamma_1, \Gamma_1}\right), \{\mu_k\}_1^{N_r-2} := \text{sp}(S^*) \text{ and } \{\beta_k\}_1^{N_r-2} := \text{sp}(B),$$

we obtain for the eigenvalues⁴ λ_k of MB the formula

$$\lambda_k = \frac{\gamma_k + \mu_k}{1 + \gamma_k \alpha_k} \beta_k. \tag{11}$$

Hence, in this special case, both *NumOpt* and *FracOpt* give identical result, namely $\gamma_k = -\mu_k$! This is *atypical* for OSMs, see [5, 11], but is due to the fact that there is no interaction between the choices of γ_k for different k due to orthogonality. We show this in Figure 2.

We note that in this case (7) is overestimating but its minimizer solves (6) as well, i.e., *the method itself is optimized, just the bound is not sharp*.

For arbitrary vectors $\mathbf{v}_1, \dots, \mathbf{v}_r \in \mathbb{R}^{N_r-2}$ in (9), even a rank one approximation now can interact with all of the eigenmodes, and $\|MB\|$ cannot be easily evaluated: we obtain the formula

$$W^T MBW = \begin{bmatrix} \alpha_1 & & \\ & \ddots & \\ & & \alpha_{N_r-2} \end{bmatrix}^{-1} \left[\begin{bmatrix} \alpha_1 & & \\ & \ddots & \\ & & \alpha_{N_r-2} \end{bmatrix} + \hat{S} \right]^{-1} \left(\hat{S} + \begin{bmatrix} \mu_1 & & \\ & \ddots & \\ & & \mu_{N_r-2} \end{bmatrix} \right) \begin{bmatrix} \beta_1 & & \\ & \ddots & \\ & & \beta_{N_r-2} \end{bmatrix}$$

³ The Schur complement converges to a Green's function when the mesh is refined, and the Green's function for Laplace's equation has a diagonal singularity, see [6, Section 5.3, Remark 16 and below].

⁴ Since MB is diagonalized by W , it is symmetric and thus the eigenvalues correspond to the singular values up to a sign.

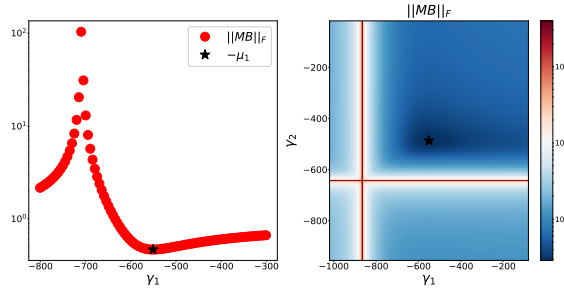


Fig. 2: $\|MB\|_F$ for the parameters γ_i close to the eigenvalues of S^* for $r = 1$ (left) and for $r = 2$ (right), with $NumOpt$ $\gamma_i = -\mu_i$ highlighted by \star .

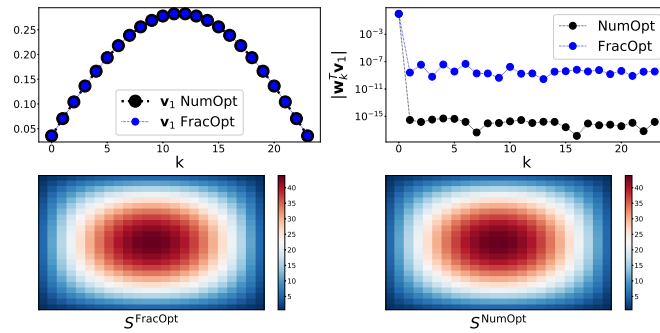


Fig. 3: $NumOpt$ and $FracOpt$ for $N_r = 26$, $L = h$ and $r = 1$. Top: coordinates of the resulting normalized vector \mathbf{v} in the basis W . Bottom: corresponding transmission matrices S^{NumOpt} , $S^{FracOpt}$.

with $\hat{S} = W^T S W$, and the denominator and numerator are given as two different diagonal matrices with the same rank- r modification. Recalling [7, Theorem 8.5.3] for $r = 1$, a lengthy but direct calculation gives that the matrices can be diagonalized with the same transformation if and only if (10) holds. Using therefore numerical optimization⁵, extensive experiments showed that $NumOpt$ and $FracOpt$ lead to the same optimal value *numerically*, for an example, see Figure 3. Again for (6) *the minimizer is not unique* but offers a sharper estimate on the convergence factor, and, in spite of having a worse bound in (7), the actual minimizer also solves the 2-norm problem in (6) and thus only the bound is affected, not the method. These observations remained consistent changing any meaningful parameters of both the problem and the various optimization routines.

We next investigate hierarchical matrices which are well suited to approximate the singularity appearing on the diagonal of the Schur complement for elliptic problems [1], and which were proposed for transmission for Helmholtz problems in [3]. Hierarchical matrices were developed to approximate directly in norm, corre-

⁵ We used the routine `scipy.optimize()` with the option `shgo` (see [2]) for global optimization and options `Nelder-Mead` and `BFGS` for local optimization.

sponding to *NumOpt*, and in practice this might be sufficient due to the astounding accuracy *and* efficiency of the hierarchical formats, see our example at the end. We study whether *NumOpt* and *FracOpt* are equivalent also for hierarchical matrices. The eigenvalue theory for hierarchical matrices focuses on localization of eigenvalues through iterative processes, see ,e.g., [9] and references therein. The explicit computation of $\|MB\|$ is hence out of reach, and we focus on numerical exploration.

We consider the simplest setting – a one-level hierarchy with the HODLR format⁶ and we assume $N_r = 2n$ for some $n \in \mathbb{N}$. Taking a 2-by-2 blocking of S ,

$$S = \begin{bmatrix} S^1 & S_{\text{off-diag}} \\ S_{\text{off-diag}}^T & S^2 \end{bmatrix}, \quad \text{with } S^1, S^2, S_{\text{off-diag}} \in \mathbb{R}^{n \times n},$$

the minimization problem (7) is posed over S with S^1 and S^2 equal to their counterparts in S^* and with $S_{\text{off-diag}}$ of rank r . As S^* is persymmetric, so are its off-diagonal blocks, and taking J as the exchange matrix⁷, we observe that $S_{\text{off-diag}}^* J$ is symmetric and thus permits a symmetric low-rank approximation of the form (9)⁸. Letting $\mathbf{q}_1, \dots, \mathbf{q}_r$ be the eigenvectors of S^* , we first consider

$$S_{\text{off-diag}} J = \sum_{i=1}^r \gamma_i \mathbf{q}_i \mathbf{q}_i^T, \quad (12)$$

where $\gamma_i \in \mathbb{R} \setminus \{0\}$. In our numerical experiments now *FracOpt* outperformed *NumOpt* slightly. For $N_r = 26$, $L = h$ and $r = 1$ *FracOpt* converges 6% faster than *NumOpt*⁹. This drops even lower for $r > 1$ (as the off-diagonal blocks are low-rank, e.g., $r = 2$ gives 2%) and seems to be quite stable under mesh refinement ($N_r = 52$ gives 10%, $N_r = 258$ gives 13%). For (6) instead of (7), we observe better bounds but with the same tendencies when changing r or N_r . We show the results for $r = 1, 2$ in Figure 4. Comparing to the global low-rank case, the situation *qualitatively* changed, as there is an improvement going from *NumOpt* to *FracOpt*.

For a more general set of vectors,

$$S_{\text{off-diag}} J = \sum_{i=1}^r \gamma_i \mathbf{v}_i \mathbf{v}_i^T, \quad (13)$$

with $\mathbf{v}_1, \dots, \mathbf{v}_r \in \mathbb{R}^n$ normalized and linearly independent, the *FracOpt* approach gives again a minimizer $S_{\text{off-diag}}^{\text{FracOpt}}$ that is suboptimal in terms of approximating $S_{\text{off-diag}}^*$, but minimizes $\|MB\|_F$ better than $S_{\text{off-diag}}^{\text{NumOpt}}$. For $r = 1$ we show a rep-

⁶ Standing for *hierarchical off-diagonal low-rank*.

⁷ The matrix with ones on the anti-diagonal and zeros elsewhere.

⁸ The low-rank approximation of $S_{\text{off-diag}}$ can then be directly reconstructed from the one of $S_{\text{off-diag}} J$ by observing that $J = J^{-1}$.

⁹ This refers to the improvement of the bound (5), e.g., *FracOpt* converging 6% faster than *NumOpt* means $(\|M^{\text{NumOpt}} B\|_F)^{1.06} = \|M^{\text{FracOpt}} B\|_F$.

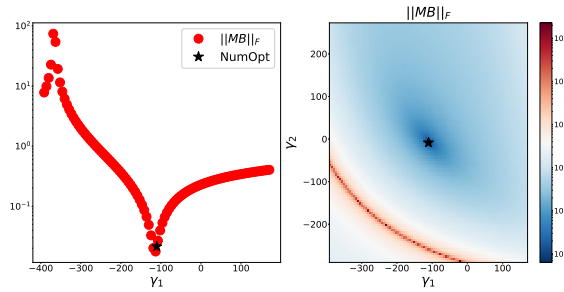


Fig. 4: $\|MB\|$ for the parameters γ_i of the off-diagonal block $S_{\text{off-diag}}J$ close to the eigenvalues of that block for $r = 1$ (left) and for $r = 2$ (right), with the $NumOpt$ result for γ_i highlighted by \star .

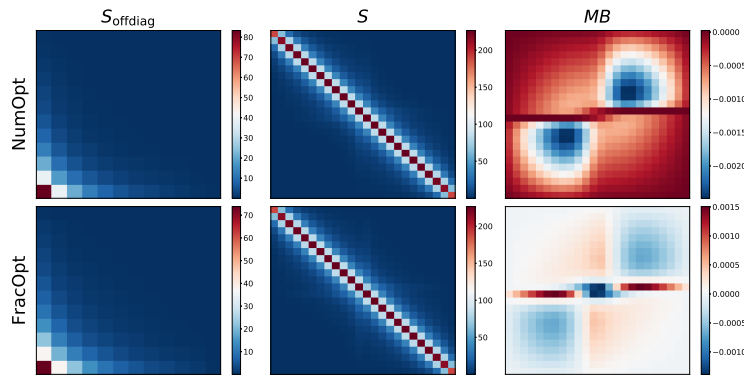


Fig. 5: Comparison of $NumOpt$ (top) and $FracOpt$ (bottom) for $N_r = 26$, $L = h$ and $r = 1$. We show S_{offdiag} (left), then S (middle) and then MB (right). Although the difference in the second column seems to be almost negligible, its effect on MB is clearly visible.

representative example¹⁰ in Figure 5. For $N_r = 26$, $L = h$ and $r = 1$, $FracOpt$ converges approximately 25% faster than $NumOpt$ – in terms of the bound. This observation is in alignment with the performance, see Figure 6 later on. Taking $r > 1$ again diminishes this improvement (with $r = 2$ we get 13%) but refining h increases the improvement (with $N_r = 52$ we get 43%) – in contrast to the previous setting. We also observed that (6) and (7) now give different minimizers, which are comparable in both the bound and the method performance ((7) is slightly worse). In the context of OSMs, the optimization gains are quite small, see, e.g., [4, Section 3.4]. Thus, we observe that $FracOpt$ and $NumOpt$ are no longer equivalent for hierarchical formats but they seem to perform comparably for our model problem.

Finally, we show a numerical comparison of the iterative solver performance, including a full hierarchical approximation of S^* in the formats HODLR and \mathcal{H}_2 in Figure 6 (the full formats correspond to $NumOpt$; for more details see [8, Figure 2.1 and 2.3] and references therein). We see that simple low rank approximations of

¹⁰ In the sense that mesh refinement only refines these results but does not change their “shape”.

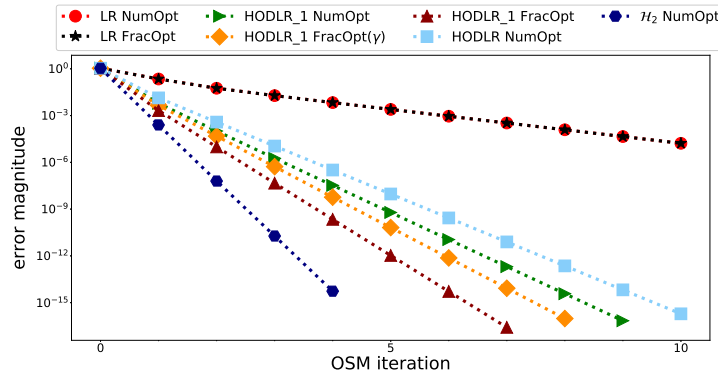


Fig. 6: Convergence of POSM for different choices of S . LR denotes the global low-rank, HODLR_1 the one-level HODLR format and FracOpt(γ), FracOpt denote the two variants (12) and (13) (we omit this for the global low-rank as there is numerically no difference in these). HODLR, \mathcal{H}_2 are \mathcal{H} -matrix formats corresponding to a binary partitioning with weak and standard admissibility conditions, see [8, Figure 2.1 and 2.3]. We take $N_r = 26$, $L = h$ and $r = 1$ wherever applicable.

the entire Schur complement can not perform very well as they miss the diagonal singularity. Hierarchical formats perform well, and follow our theoretical results.

References

1. Bebendorf, M., Hackbusch, W.: Existence of \mathcal{H} -matrix approximants to the inverse FE-matrix of elliptic operators with L^∞ -coefficients. *Numerische Mathematik* **95**(1), 1–28 (2003)
2. Endres, S.C., Focke, W.W., Sandrock, C.: A simplicial homology algorithm for Lipschitz optimisation. *Journal of Global Optimization* **72**(2), 181–217 (2018)
3. Engquist, B., Ying, L.: Sweeping preconditioner for the Helmholtz equation: Hierarchical matrix representation. *Communications on Pure and Appl. Math.* **64**, 697–735 (2011)
4. Gander, M.J.: Optimized Schwarz methods. *SIAM J. on Numer. Anal.* **44**(2), 699–731 (2006)
5. Gander, M.J., Loisel, S., Szyld, D.B.: An optimal block iterative method and preconditioner for banded matrices with applications to PDEs on irregular domains. *SIAM Journal on Matrix Analysis and Applications* **33**(2), 653–680 (2012)
6. Gander, M.J., Zhang, H.: A class of iterative solvers for the Helmholtz equation: factorizations, sweeping preconditioners, source transfer, single layer potentials, polarized traces, and optimized Schwarz methods. *SIAM Review* **61**(1), 3–76 (2019)
7. Golub, G.H., van Loan, C.F.: *Matrix Computations*, Third edn. Johns Hopkins University Press, Baltimore (1996)
8. Hackbusch, W., Khoromskij, B.N., Kriemann, R.: Hierarchical matrices based on a weak admissibility criterion. *Computing* **73**(3), 207–243 (2004)
9. Mach, T.: Eigenvalue algorithms for symmetric hierarchical matrices. Ph.D. thesis, Chemnitz University of Technology (2012)
10. St-Cyr, A., Gander, M.J., Thomas, S.J.: Optimized multiplicative, additive, and restricted additive Schwarz preconditioning. *SIAM Journal on Scientific Computing* **29**(6), 2402–2425 (2007)
11. Vanzan, T.: Domain decomposition methods for multiphysics problems. Ph.D. thesis, University of Geneva (2020)